Coherent Control of Total Transmission of Light through Disordered Media

S. M. Popoff, A. Goetschy, S. F. Liew, A. D. Stone, and H. Cao*
Department of Applied Physics, Yale University, New Haven, Connecticut 06511, USA
(Received 4 August 2013; published 1 April 2014)

We demonstrate order of magnitude coherent control of total transmission of light through random media by shaping the wave front of the input light. To understand how the finite illumination area on a wide slab affects the maximum values of total transmission, we develop a model based on random matrix theory that reveals the role of long-range correlations. Its predictions are confirmed by numerical simulations and provide physical insight into the experimental results.

DOI: 10.1103/PhysRevLett.112.133903 PACS numbers: 42.25.Bs, 02.10.Yn, 05.60.Cd

A lossless strong scattering medium that has a thickness L much larger than the elastic mean free path ℓ is normally opaque to incident beams of light, with a small fraction ℓ/L of the incident photon flux diffusively transmitted. However, it has been known for over two decades that, due to the coherence of elastic scattering, this transmitted flux is not totally random in character, but has subtle correlations that were first discovered in the context of mesoscopic electron transport [1–4]. One striking implication of these correlations is that an optimally prepared coherent input beam could be transmitted through a scattering medium hundreds of mean free paths in thickness with order unity efficiency. These highly transmitting input states are eigenvectors of the matrix $t^\dagger t$, where t is the transmission matrix (TM) of the sample. They were predicted using a random matrix theory approach [1–3] and were termed "open channels."

Because the input electron states are not controllable in mesoscopic conductors, the open channel concept was not testable there, except indirectly through other properties such as conductance fluctuations or shot noise [5]. Experimental measurements of the TM through disordered waveguides at microwave frequencies are consistent with the theory developed for this geometry [6–8] and imply that open channels should exist, but enhanced transmission has not yet been directly demonstrated in these systems due to the difficulty of imposing an appropriate input waveform. The advent of wave front shaping methods using a spatial light modulator (SLM) at optical frequencies has reopened the search for this dramatic effect in strong scattering media. It has already been shown that wave front shaping of input states combined with feedback optimization can enable diverse functions for multiple scattering media in optics [9], causing them to act as lenses [10,11], phase plates [12,13], or spectral filters [14,15]. However, coherent control of total transmission, which is a nonlocal property of the TM, is much more difficult. Some progress in this direction has been made by studying the increase of the total transmission when focusing light through scattering media to wavelength scale spots [16] or by measuring the partial TM and injecting light into calculated singular vectors [17]. In addition, a recent study highlights effects of the mesoscopic correlations on the transmission properties by measuring a large TM [18]. We report here a further significant step: order of magnitude variation of total transmission through a strong scattering medium with average transmission ~5%. We show that such dramatic variations are only possible because of significant mesoscopic correlations in the diffusive transmission.

Until recently the theory underlying the prediction of open channels assumed full coherent control of all input channels, which is in principle possible in the waveguide geometry used in microwave experiments [6–8]. This is not achievable in optical experiments, which usually have limited numerical aperture (excluding some input wave vectors), and also are based on incidence of a finite-cross-section beam on a wide slab. Such a setup, however, is widely used in many practical applications. Recently, it was shown theoretically how to calculate the distribution of the "transmission eigenvalues" (the eigenvalues of $t^\dagger t$) and the maximum transmission enhancement in the presence of incomplete channel control [19]. Loss of control reduces the possible transmission enhancement, eventually causing the TM to lose the mesoscopic correlations and behave like an uncorrelated Gaussian random matrix, whose singular value density follows the Marcenko-Pastur (MP) law [11,20,21]. Thus it is essential to calculate the channel control parameters for a realistic experimental setup, so as to determine the maximum transmission enhancement possible. However, the theory of Ref. [19], while it does describe the effect of finite numerical aperture, did not address the geometry of a finite illumination area used in optical experiments, in which the light diffuses outwards in the transverse direction at the same time as it penetrates the sample. We present a quantitative theoretical solution to this important problem in coherent diffusion, showing that for a finite illumination area in an open geometry the transmission eigenvalue density does belong to the family of distributions derived in Ref. [19], with an effective channel control parameter, which depends on the long-range

mesoscopic correlations, and can be calculated microscopically with no fitting parameter.

To control total transmission through a disordered slab, we designed an experiment to achieve a high degree of control of the phase of the input light with both polarizations. The illumination area on the slab surface is much larger than the wavelength. The experimental apparatus is presented in Fig. 1(a) and detailed in the Supplemental Material [22]. The modulated wave front is projected onto the pupil of a microscope objective of numerical aperture 0.95. Adjacent pixels of the SLM are grouped to form "macropixels," whose size determines the illumination area on the sample. In order to collect light in all output channels, we place the sample directly onto a large photodetector. This allows us to measure the total transmitted light without being limited by the numerical aperture of the collecting optics. Two additional photodetectors are used to measure the incident light intensity before the microscope objective and the reflection from the sample. We then perform a feedback optimization procedure similar to the sequential algorithm developed in Ref. [10] to increase or decrease the total transmission. The value to maximize or minimize is the ratio of the total integrated transmitted intensity over the input intensity, henceforth termed the total transmission T. It is crucial to optimize the ratio, because wave front shaping by the SLM modifies not only the transport of light through the sample, but also the transmission of the optical system that delivers light from the SLM to the sample, and is, hence, vulnerable to systematic errors or artifacts [23].

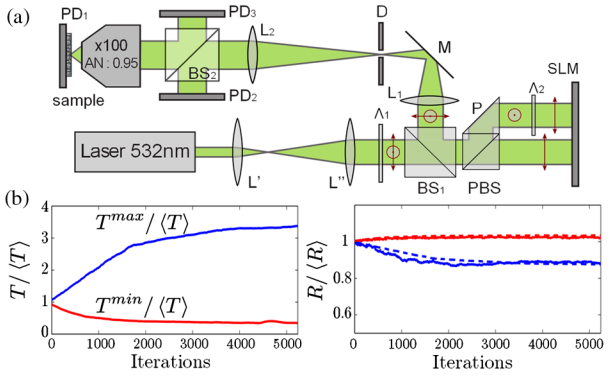

FIG. 1 (color online). (a) Schematic of the experimental setup for the control of total transmission. As detailed in the Supplemental Material [22], the two polarizations of a Nd:YAG laser, $\lambda = 532$ nm, are modulated by two different areas of a phase-only SLM. The scattering sample is placed at the focal plane of the objective. Three photodetectors, PD_1, PD_2, and PD_3, measure, respectively, the intensities of transmitted, incident, and reflected light. (b) Measured $T/\langle T\rangle$ (left panel) and $R/\langle R\rangle$ (right panel) versus the optimization step for enhancement (increasing blue curve) and reduction (decreasing red curve) of the total transmission. The sample is 20 μm thick, and the average transmission $\langle T\rangle \sim 5\%$. The dotted line represents the reflection estimated from the transmission using $R/\langle R\rangle = (1-T)/(1-\langle T\rangle)$.

The scattering samples are slabs of randomly packed polydisperse TiO_2 microparticles of median diameter 410 nm, deposited on glass cover slips by evaporation. The mean free path, measured from a coherent backscattering experiment, is $\ell = 0.8 \pm 0.1$ μm. To demonstrate coherent control we both maximize and minimize T. In Fig. 1(b) we show results for a sample of average transmission $\langle T\rangle \sim 5\%$ that demonstrate an enhancement of $T \sim 3.6$, and a reduction ~ 3.1. Thus, the total transmission of a single realization of a scattering medium can be tuned by more than a factor of 11 between 1.6% and 18%. The diameter of the illumination area on the sample surface is 8.3 μm, and the number of macropixels of the SLM, whose phases are optimized, is $N_{\text{in}} = 1740$. We also measure the change in reflection R (ratio of the reflected light intensity over the incident intensity), and compare it to the change estimated from the transmission using the relation $R/\langle R\rangle \simeq (1-T)/(1-\langle T\rangle)$ [Fig. 1(b)]. The good agreement confirmed that the variations of the measured total transmission are due to changes of the total transmission through the scattering sample (further verifications are considered in the Supplemental Material [22]).

We show in the following that mesoscopic correlations are essential to the significant variation of total transmission. We compare our data to the predictions of the uncorrelated random matrix ensemble. For an uncorrelated TM described by the MP law, the mean maximum transmission satisfies [20]

$$\frac{\langle T^{\max}\rangle}{\langle T\rangle} = (1+\sqrt{\gamma})^2, \tag{1}$$

where γ is the ratio of the number of controlled input channels to the number of excited output channels. A reasonable estimate is $\gamma \simeq (D/D_{\text{out}})^2$, where D_{out} is the typical size of the diffusive output spot. The maximum possible transmission (1) is monotonically decreasing with the sample thickness L because D_{out} increases with L for fixed input illumination diameter D. In Fig. 2(a) we plot $T^{\max}/\langle T\rangle$ measured versus L for a fixed D, finding that instead of decreasing, it increases and then saturates at the largest L shown. The value of the enhancement at the largest L is more than twice that of the MP law. Similarly, for fixed L and variable D, the data in Fig. 2(b) show much higher enhancements than the predictions of the uncorrelated model, implying that significant correlations in the TM enable larger coherent control of transmission.

To further confirm this, we intentionally spoil the correlations by increasing the illumination diameter, which increases the total number of input channels N_{tot}, but without increasing the number of controlled input channels N_{in}. This should reduce the transmission enhancement towards the MP value. We first use an illumination diameter

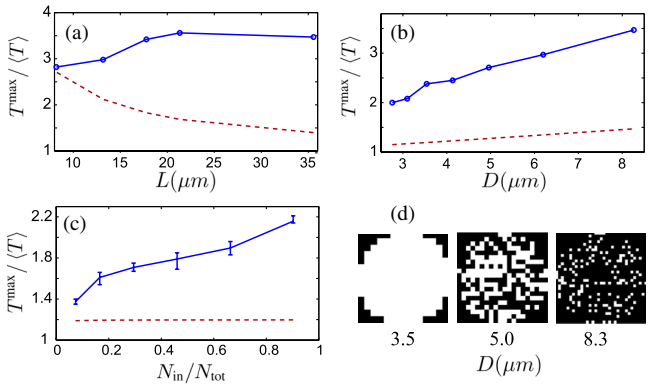

FIG. 2 (color online). Enhancement of transmission as a function of the sample thickness L for an illumination diameter of $D = 8.3$ μm (a) and as a function of the input illumination diameter D for a fixed sample thickness $L = 23$ μm (b). Experimental data are shown by blue dots, the estimation by Eq. (1) in red dotted lines. (c) $T^{max}/\langle T\rangle$ as a function of the fraction of controlled input channels N_{in}/N_{tot}. Experimental data are blue dots with the error bars from ensemble measurements; the dotted red curve represents the prediction of Eq. (1) for uncorrelated systems. (d) Representative amplitude patterns of the SLM macropixels for three illumination diameters D. The dark macropixels are switched off.

of 3.6 μm and run the optimization algorithm controlling all 460 independent macropixels on the SLM. Then we increase progressively the illumination diameter to 12.4 μm by shrinking the macropixels and run the optimization process using only $N_{in} = 460$ randomly selected independent macropixels. We present in Fig. 2(d) schematics of the SLM patterns for three illumination diameters D. The uncontrolled macropixels are switched off by printing a high spatial frequency pattern on the SLM. $\langle T^{max}\rangle/\langle T\rangle$ is plotted in Fig. 2(c) versus the fraction of controlled input channels N_{in}/N_{tot}. Incomplete channel control progressively suppresses the effect of mesoscopic correlations and the enhancement of total transmission decreases continuously. When only a small fraction of the macropixels is chosen, they are nearly independent. Consequently, $\langle T^{max}\rangle/\langle T\rangle$ becomes comparable to the value from the uncorrelated model.

To get a quantitative understanding of the previous results, we develop a theoretical model for the transmission eigenvalue density that takes into account the effects of an arbitrary input intensity profile and is valid for an open slab as well as for a waveguide geometry. Since the maximal total transmission is equal to the highest transmission eigenvalue, this theory will give us access, in particular, to $\langle T^{max}\rangle$. For this purpose, we use the filtered random matrix (FRM) ensemble, recently introduced to describe the role of incomplete channel control in experiments [19]. Applying the FRM equations to the study of the transmission matrix, the authors calculated the eigenvalue density of the matrix $\tilde{t}^{\dagger}\tilde{t}$, where $\tilde{t}$ is the filtered TM, with only a fraction m_1 (m_2) of the input (output) channels controlled (measured). The eigenvalue distribution is determined by three parameters, m_1, m_2, and the mean transmission eigenvalue $\bar{\tau}$. An important assumption of the model is that all channels in the TM, whether measured or not, play an equivalent "role" with respect to the scattering process. This is always true for channels represented by waveguide modes or plane waves which diffuse equivalently inside the sample. Hence, the model can be applied to a wide slab illuminated over its entire surface with a finite numerical aperture (k-space filtering), which has been confirmed by the agreement of the theory with numerical simulations [19].

In general, the previous assumption does not hold for spatial filtering arising from a finite illumination area, for which there is an outwards spreading diffusion halo, and points at the edge of the input area are not equivalent to those in the middle. It was thus an open question as to whether the transmission eigenvalue density for this geometry corresponds to the FRM distribution, with effective parameters m_1 and m_2. We focus on our current experimental setup in which essentially all of the output light was collected ($m_2 \simeq 1$). Extensive simulations of this configuration (described below) revealed that it does lead to a transmission eigenvalue density described by the FRM distribution, with an effective value of the input parameter m_1 and with $m_2 = 1$. A property of this FRM distribution is that m_1, normally considered as an experimental parameter, is also given by [19]

$$m_1 = \frac{\mathrm{Var}(\tilde{\tau})}{\mathrm{Var}(\tau)}, \tag{2}$$

where τ and $\tilde{\tau}$ are the eigenvalues of $t^{\dagger}t$ and $\tilde{t}^{\dagger}\tilde{t}$, respectively. Equation (2) allows us to define the effective channel fraction m_1 for our experiment, since we do not know *a priori* how to extract it from the geometric parameters D, L. In the Supplemental Material [22] we confirm numerically, from direct solution of the wave equation in 2D and 3D, that Eq. (2) gives the correct value of m_1 to predict numerically generated transmission eigenvalue densities for our setup of a wide slab with finite illumination area. The numerical method is the same as was used to generate the data shown in Figs. 3 and 4 (described below).

Having established numerically that Eq. (2) determines the desired eigenvalue density, we can formulate an analytic theory for this quantity using the diagrammatic methods developed for coherent wave transport [4,24]. Using $\mathrm{Var}(\tau) = 2\bar{\tau}/3 - \bar{\tau}^2$, and decomposing $\langle\tilde{\tau}^2\rangle$ as the product of four Green's functions of the wave equation, we show in the Supplemental Material [22] that the effective control parameter m_1 can be accurately expressed as

$$m_1 = \frac{1}{1 - 3\bar{\tau}/2}\left[\int d\mathbf{q}\rho(\mathbf{q})\frac{I(\mathbf{q})I(-\mathbf{q})F(\mathbf{q})}{I(\mathbf{0})F(\mathbf{0})} - \frac{3\bar{\tau}^2}{2}\right], \tag{3}$$

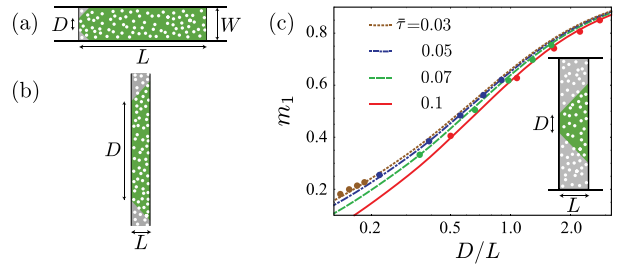

FIG. 3 (color online). (a),(b) Geometries for which the fraction of controlled channels m_1 is given by a simple analysis of the input field (see text). (c) Effective fraction of controlled channel (2) in the geometry relevant for our optical experiment. Numerical results (dots) are obtained from the simulation of the wave equation in a two-dimensional disordered slab, for different values of the illumination diameter D and the slab thickness L. The dielectric function is $\epsilon(\mathbf{r}) = n_0^2 + \delta\epsilon(\mathbf{r})$, with $n_0 = 1.3$ and $\delta\epsilon(\mathbf{r})$ uniformly distributed between $[-1.02, 1.02]$ in the slab and $\delta\epsilon(\mathbf{r}) = 0$ outside the slab. The four sets of points correspond to $kL = 120$, 187, 280, 450. The solid lines represent the theoretical prediction (3), where $I(\mathbf{q}) = D\mathrm{sinc}(qD/2)$.

where $\rho(\mathbf{q}) = \sum_n \delta(\mathbf{q} - \Delta\mathbf{q}_n)/A$ is the density of transverse states spacings $\Delta\mathbf{q}_n$ per unit area $A = W^{d-1}$ (d is the space dimension and W is the transverse dimension, $W \to \infty$ in free space), $I(\mathbf{q})$ is the Fourier transform of the transverse input intensity profile, and $F(\mathbf{q})$ is the kernel that gives rise to the long-range correlation of the speckle pattern, which is described by the C_2 correlation function (see the Supplemental Material [22] and Ref. [24]). More specifically, the correlation between the total transmission associated with two channels with transverse momenta $\mathbf{q}_a$ and $\mathbf{q}_a + \mathbf{q}$ is $C_2(\mathbf{q}) = F(\mathbf{q})/g$, where $g = \langle \mathrm{Tr}(t^\dagger t)\rangle$. Its long-range character is due to interference of pairs of diffusive paths that interact through a Hikami vertex with a probability $1/g$. The effect of the finite illumination area is taken into account by the factor $I(\mathbf{q})I(-\mathbf{q})/I(\mathbf{0})$ in Eq. (3), which arises because the four input channels involved in

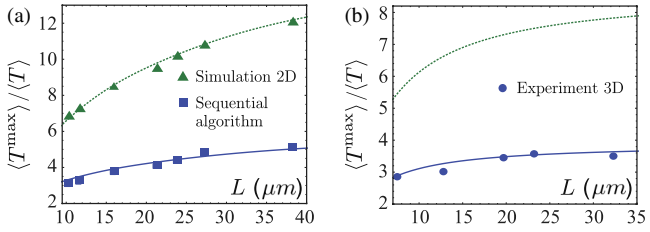

FIG. 4 (color online). Maximal transmission in a slab of thickness L, illuminated with $D = 16\lambda$. (a) 2D simulations (dots), calculated with the same parameters as in Fig. 3, are compared with the theoretical prediction (solid and dashed lines) based on Eqs. (4) and (3). The effect of the finite number of modes is taken into account, as detailed in the Supplemental Material [22], and the effect of the sequential algorithm (blue squares) is included in the theory through the substitution $m_1 \to \alpha m_1$, with $\alpha \simeq 0.26$. (b) The 3 D experiment (dots) is well described by Eq. (4), where $m_1 \to \alpha m_1$, with m_1 given by Eq. (3) solved in 3D and α identical to the 2D case.

$\langle \tilde{\tau}^2\rangle$ have different weights due to spatial variation of the input beam. The three terms, $\rho(\mathbf{q})$, $I(\mathbf{q})$, and $F(\mathbf{q})$, have distinct length scales, $1/W$, $1/D$, and $\max(1/L, 1/W)$, respectively. They lead to different expressions for m_1 in different situations.

In the case of a quasi-one-dimensional waveguide [$W \ll L$, Fig. 3(a)] with a lossless reflecting boundary, only the $\mathbf{q} = \mathbf{0}$ component is selected by the density of states, leading to a simple geometrical result, $m_1 \simeq (D/W)^{d-1}$. The situation is very different in an optics experiment with a wide slab [$W \to \infty$ and $\rho(\mathbf{q}) = 1/(2\pi)^{d-1}$]. If the slab is illuminated with an area of diameter D much larger than the sample thickness L [Fig. 3(b)], only the term $F(\mathbf{0}) = 2/3$ contributes, and one finds $m_1 \to 1$, consistent with the physical picture that if the transverse diffusion is negligible in crossing the sample then all channels are equivalent and controlled. However, if $D \lesssim L$ [inset of Fig. 3(c)], all components $\mathbf{q} \neq \mathbf{0}$ of $F(\mathbf{q})$ contribute to the result (3), meaning that the effective fraction of controlled channels is not simply given by geometrical considerations based on the diffusion equation, but originates from wave interference that leads to long-range correlations. Further analysis of the wide slab case gives an m_1 that is essentially determined by the ratio D/L, with small corrections due to $\bar{\tau} \propto \ell/L$ that vanish in the limit $\bar{\tau} \to 0$. In the limit $\ell \ll D \ll L$, we find the striking result that $m_1 \sim (D/L)\ln(L/D)$ in 2D and $m_1 \sim D/L$ in 3D. In particular, the loss of control in 3D does not decrease as the ratio of the input and output areas as one might expect from an analysis based only on the diffusion equation, and, hence, the possible transmission enhancement in 3D is parametrically larger than expected.

To test the validity of the prediction (3), we studied numerically the transmission matrix of a two-dimensional disordered slab embedded in a multimode waveguide, using the recursive Green's function method [25]. The waveguide is wide enough that the diffusion halo at the output never reaches side walls. We compare in Fig. 3 the numerical results (2), averaged over 100 configurations, with the analytic expression (3), for four different slab thicknesses and five different illumination areas, finding excellent agreement.

Finally, once the value of m_1 is known, the full distribution of transmission eigenvalues follows from the FRM equations [19], which allows us to calculate the maximal transmission enhancement possible for a given m_1. $\langle T^{\max}\rangle$ is given by the upper edge of the support of the eigenvalue density:

$$\langle T^{\max}\rangle = f^{\max}(m_1, m_2 = 1, \bar{\tau}), \tag{4}$$

where the expression for $f^{\max}$ is given in Ref. [19].

The analytic predictions for the transmission enhancement given by Eqs. (4) and (3) are confirmed by simulations in a 2D slab with excellent agreement [Figs. 3(c) and 4(a)]. However the experiments use sequential search, phase-only

optimization, which is not expected to find the global optimum predicted from the theory. We estimate from 2D simulations of sequential phase-only optimization that m_1 is effectively reduced to αm_1 with $\alpha \simeq 0.26$, and apply the same reduction factor to the 3D results to compare with the experiment (for which simulations are computationally unfeasible), finding rather good agreement (see Fig. 4). This suggests that the maximal enhancement of total transmission achieved for the samples in our experiment is limited mainly by the optimization procedure, instead of other effects such as noise in the measurements or instability of the setup.

We thank Yaron Bromberg, Brandon Redding, Sylvain Gigan, and Allard Mosk for useful discussions. This study was supported in part by the facilities and staff of the Yale University Faculty of Arts and Sciences High Performance Computing Center. This work is funded by the NSF Grant No. ECCS-1068642.

*hui.cao@yale.edu

[1] O. N. Dorokhov, Solid State Commun. **51**, 381 (1984).
[2] P. A. Mello, P. Pereyra, and N. Kumar, Ann. Phys. (N.Y.) **181**, 290 (1988).
[3] Y. V. Nazarov, Phys. Rev. Lett. **73**, 134 (1994).
[4] E. Akkermans and G. Montambaux, *Mesoscopic Physics of Electrons and Photons* (Cambridge University Press, Cambridge, England, 2007).
[5] C. W. J. Beenakker, Rev. Mod. Phys. **69**, 731 (1997).
[6] M. Stoytchev and A. Z. Genack, Phys. Rev. Lett. **79**, 309 (1997).
[7] Z. Shi and A. Z. Genack, Phys. Rev. Lett. **108**, 043901 (2012).
[8] M. Davy, Z. Shi, J. Wang, and A. Z. Genack, Opt. Express **21**, 10367 (2013).
[9] I. Freund, Physica (Amsterdam) **168A**, 49 (1990).
[10] I. M. Vellekoop and A. P. Mosk, Opt. Lett. **32**, 2309 (2007).
[11] S. M. Popoff, G. Lerosey, R. Carminati, M. Fink, A. C. Boccara, and S. Gigan, Phys. Rev. Lett. **104**, 100601 (2010).
[12] Y. Guan, O. Katz, E. Small, J. Zhou, and Y. Silberberg, Opt. Lett. **37**, 4663 (2012).
[13] J. Park, C. Park, H. Yu, Y. Cho, and Y. K Park, Opt. Express **20** 17010 (2012).
[14] J. Park, C. Park, H. Yu, Y. Cho, and Y. K Park, Opt. Lett. **37**, 3261 (2012).
[15] E. Small, O. Katz, Y. Guan, and Y. Silberberg, Opt. Lett. **37**, 3429 (2012).
[16] I. M. Vellekoop and A. P. Mosk, Phys. Rev. Lett. **101**, 120601 (2008).
[17] M. Kim, Y. Choi, C. Yoon, W. Choi, J. Kim, Q.-H. Park, and W. Choi, Nat. Photonics **6**, 583 (2012).
[18] H. Yu, T. R. Hillman, W. Choi, J. O. Lee, M. S. Feld, R. R. Dasari, and Y. K. Park, Phys. Rev. Lett. **111**, 153902 (2013).
[19] A. Goetschy and A. D. Stone, Phys. Rev. Lett. **111**, 063901 (2013).
[20] V. A. Marčenko and L. A. Pastur, Mathematics of the USSR Sbornik **1**, 457 (1967).
[21] A. Aubry and A. Derode, Phys. Rev. Lett. **102**, 084301 (2009).
[22] See Supplemental Material at http://link.aps.org/supplemental/10.1103/PhysRevLett.112.133903 for a full description of the setup, a detailed study of the presence of optical artefacts, a numerical verification of the validity of Eq. (2) and the proof of Eq. (3).
[23] S. M. Popoff, A. Aubry, G. Lerosey, M. Fink, A. C. Boccara, and S. Gigan, Phys. Rev. Lett. **107**, 263901 (2011).
[24] M. C. W. van Rossum and T. M. Nieuwenhuizen, Rev. Mod. Phys. **71**, 313 (1999).
[25] H. U. Baranger, D. P. DiVincenzo, R. A. Jalabert, and A. D. Stone, Phys. Rev. B **44**, 10637 (1991).